

# ASSESSMENT OF WELDING RESIDUAL STRESSES IN RECTANGULAR PLATES USING VIBRATION DATA

## Alberto Borges Vieira Júnior

Universidade Federal de Uberlândia, Campus Santa Mônica, Bloco 1M, Uberlândia, MG, 38400-902  
abvieira@mecanica.ufu.br

## Américo Scotti

Universidade Federal de Uberlândia, Campus Santa Mônica, Bloco 1M, Uberlândia, MG, 38400-902  
ascotti@mecanica.ufu.br

## Domingos Alves Rade

Universidade Federal de Uberlândia, Campus Santa Mônica, Bloco 1M, Uberlândia, MG, 38400-902  
domingos@ufu.br

**Abstract.** A new hybrid numerical/experimental technique for stress assessment, which explores the influence of stresses on dynamic responses of structures, is used for the identification of weld-induced residual stresses in rectangular plates. This technique, named SIFDRIM (Stress Identification from Dynamic Responses - Inverse Method), consists of using modal properties, like a set of natural frequencies, to identify the parameters of a given mode for the stress distribution over the plate. A parameterized stress model suitable to the case of welding residual stresses is presented, in terms of a differential equation that relates Airy's stress function to the plastic strains resulting from the welding process. From this stress function, the stress components  $\mathbf{s}_x$ ,  $\mathbf{s}_y$  and  $\mathbf{t}_{xy}$  (assuming plane stress state) can be assessed. To demonstrate the feasibility of the method, it is used for the assessment of stresses in a TIG (GTAW) welded thin rectangular steel plate, based on experimentally measured natural frequencies and numerically computed weld-induced stress distributions obtained from the literature.

**Keywords:** Residual stresses, Vibration of plates, Welding, Inverse problems.

## 1. Introduction

The assessment of welding residual stresses is a topic of great technological interest, since these stresses influence, to a large extent, the quality of welded manufactured parts in terms of distortion, corrosion, buckling, crack initiation and propagation and mechanical resistance (Parlane et al, 1981).

The assessment of residual stresses is often a difficult task. Existing experimental techniques of stress analysis can be divided in two groups: techniques applicable to in-service structures, and those applicable to structures tested in laboratory environment. As examples of the first group, one can cite *X-rays*, *Hole-center drilling*, *ultrasonic techniques*, *Neutron diffraction technique* and *holography*. On the other hand, techniques intended to laboratory environment are, for instance, *Extensometry*, *Photoelasticity* and *Moiré techniques*. These experimental techniques have inherent drawbacks, like being costly and time consuming, being destructive or semi-destructive (which is the case of *Hole-center drilling*, for instance). Moreover, in most cases, stress measurements are provided at one point at a time, and are often restricted to specific types of materials (such as *Transmission Photoelasticity*). Numerical prediction of residual stresses is also difficult, due to the complexity of the welding process (Radaj, 1992).

Recent works have proved that residual stresses influences the dynamic behaviour of welded structures (Kaldas and Dickinson, 1981, and Vieira Jr. et al., 2002). This characteristic indicates the possibility of using modal parameters obtained from dynamic tests (like a set of natural frequencies) to get information about the stress state within the structure. A method has been developed by the authors to perform this identification using optimization techniques to assess the parameters of a given stress model. This method has been applied to identify stress state of plates subjected to in-plane loads in both theoretical and experimental studies (Vieira Jr. and Rade, 2003). In the present work, it is investigated the use of the method for the identification of weld-induced residual stress in a thin rectangular welded plate.

## 2. Theory

Figure (1) illustrates the plate of dimensions  $L \times B \times t_h$ , being also depicted an element which is acted upon by normal and shear stress components  $\mathbf{s}_x$ ,  $\mathbf{s}_y$  and  $\mathbf{t}_{xy}$ .

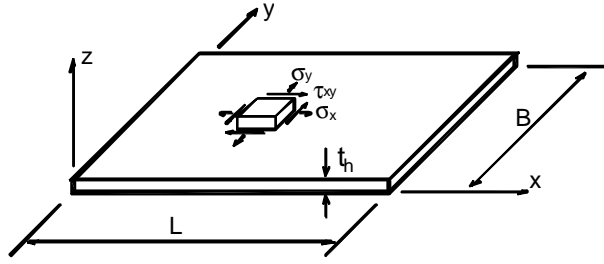


Figure 1. Plate dimensions and stress components in an element of the plate

According to Kirchhoff's theory, the following assumptions are adopted:

- plate thickness is small and constant. External faces are parallel to the middle plane (which is assumed to coincide with x-y plane);
- cross-sections remain plane and perpendicular to the middle plane;
- plane stress state is assumed, transverse shear stresses are neglected.

Neglecting dissipation effects, the Rayleigh-Ritz variational method is used to derive the eigenvalue problem associated to the flexural vibrations of the plate, taking into account the membrane stresses. With this aim, Hamilton principle is evoked:

$$\delta \int_{t_1}^{t_2} (T - V) dt = 0 \quad (1)$$

where  $T$  is the kinetic energy and  $V$  is the potential energy of the plate. These energies are given by the following expressions (Gérardin and Rixen, 1997):

$$T = \frac{1}{2} \int_S m \left( \frac{\partial w}{\partial t} \right)^2 dS \quad (2)$$

$$V = \frac{1}{2} \int_S \left\{ D \left( \frac{\partial^2 w}{\partial x^2} + \frac{\partial^2 w}{\partial y^2} \right)^2 - 2D(1 - \nu) \left[ \frac{\partial^2 w}{\partial x^2} \frac{\partial^2 w}{\partial y^2} - \left( \frac{\partial^2 w}{\partial x \partial y} \right)^2 \right] + \right. \\ \left. + t_h \left[ \mathbf{s}_x \left( \frac{\partial w}{\partial x} \right)^2 + \mathbf{s}_y \left( \frac{\partial w}{\partial y} \right)^2 + 2\mathbf{t}_{xy} \left( \frac{\partial w}{\partial x} \frac{\partial w}{\partial y} \right) \right] \right\} dS \quad (3)$$

where  $m$  indicates the mass of the plate per unit of surface,  $D = Et_h^3 / [12(1 - \nu^2)]$  is the plate flexural stiffness,  $\mathbf{s}_x$ ,  $\mathbf{s}_y$  and  $\mathbf{t}_{xy}$  designate the in-plane normal and shear stresses, respectively and  $w(x, y, t)$  represents the transverse displacements.

According to the Rayleigh-Ritz method, the plate transverse displacement field is assumed to be expressed as a truncated linear combination of arbitrarily selected admissible functions. Following the approach adopted by Kaldas and Dickinson (1981), these functions are chosen to be the eigenfunctions of vibrating beams satisfying the geometrical boundary conditions of the plate in directions  $x$  and  $y$ . Thus, one writes:

$$w(x, y, t) = \sum_{i=1}^p \sum_{j=1}^q A_{ij}(t) \mathbf{f}_i(x) \mathbf{y}_j(y) \quad (4)$$

where  $p$ ,  $q$  are the numbers of eigenfunctions considered in the truncated series in  $x$  and  $y$  directions, respectively;  $A_{ij}$  are unknown generalized coordinates and  $\mathbf{f}_i(x)$  and  $\mathbf{y}_j(y)$  designate the beam eigenfunctions.

According to Young (1950), suitable beam eigenfunctions are combinations of trigonometric and hyperbolic functions of the form:

$$\mathbf{f}_i(x) = A_i \sin\left(\mathbf{h}_i \frac{x}{L}\right) + B_i \cos\left(\mathbf{h}_i \frac{x}{L}\right) + C_i \sinh\left(\mathbf{h}_i \frac{x}{L}\right) + D_i \cosh\left(\mathbf{h}_i \frac{x}{L}\right)$$

$$\mathbf{y}_j(y) = E_i \sin\left(\mathbf{x}_i \frac{y}{B}\right) + F_i \cos\left(\mathbf{x}_i \frac{y}{B}\right) + G_i \sinh\left(\mathbf{x}_i \frac{y}{B}\right) + H_i \cosh\left(\mathbf{x}_i \frac{y}{B}\right)$$

where  $A_i, B_i, C_i, D_i, \mathbf{h}_i, E_i, F_i, G_i, H_i, \mathbf{x}_i$  are coefficients depending on the boundary conditions for the  $i$ -th vibration mode. Young(1950) provides the numerical values of these coefficients for three combinations of boundary conditions: *clamped-clamped, clamped-free* and *free-free*.

To obtain the eigenvalue problem, time-harmonic responses are assumed in (4), according to:

$$A_{ij}(t) = \bar{A}_{ij} e^{i\omega t}$$

The stationarity condition (1) is then enforced with respect to the  $p \times q$  generalized coordinates  $\bar{A}_{ij}$ , leading to the following eigenvalue problem:

$$([K] - \mathbf{I}_r [M]) \{\bar{A}_r\} = \{0\} \quad (5)$$

where the eigenvalues are related to the natural frequencies according to  $\mathbf{I}_r = \mathbf{r} t_h \mathbf{w}_r^2 L^4 / D$  and the eigenvectors  $\{\bar{A}_r\}$  are formed by the generalized coordinates  $\bar{A}_{ij}$ .

The numerical solution of equation (5) provides the natural frequencies of the plate subjected to the membrane stresses. The corresponding mode shapes can be obtained by introducing the eigenvector components  $\bar{A}_{ij}$  into (4):

$$w_r(x, y) = \sum_{i=1}^p \sum_{j=1}^q \bar{A}_{ij} \mathbf{f}_i(x) \mathbf{y}_j(y) \quad (6)$$

The general forms of the elements of matrices  $[K]_{(p \cdot q \times p \cdot q)}$  and  $[M]_{(p \cdot q \times p \cdot q)}$  are detailed in the following.

$$\begin{aligned} K_{ijrs} = & E_{ir}^{(2,2)} F_{js}^{(0,0)} + \left(\frac{L}{B}\right)^4 E_{ir}^{(0,0)} F_{js}^{(2,2)} + \mathbf{n} \left(\frac{L}{B}\right)^2 \left( E_{ir}^{(0,2)} F_{js}^{(2,0)} + E_{ir}^{(2,0)} F_{js}^{(0,2)} \right) + \\ & + 2(1-\mathbf{n}) \left(\frac{L}{B}\right)^2 E_{ir}^{(1,1)} F_{js}^{(1,1)} + \frac{t_h L^3}{DB} \int_0^L \int_0^B \left[ \mathbf{s}_x \frac{\partial \mathbf{f}_i}{\partial x} \frac{\partial \mathbf{f}_r}{\partial x} \mathbf{y}_j \mathbf{y}_s + \right. \\ & \left. + \mathbf{s}_y \mathbf{f}_i \mathbf{f}_r \frac{\partial \mathbf{y}_j}{\partial y} \frac{\partial \mathbf{y}_s}{\partial y} + \mathbf{t}_{xy} \left( \mathbf{f}_i \frac{\partial \mathbf{f}_r}{\partial x} \frac{\partial \mathbf{y}_j}{\partial y} \mathbf{y}_s + \frac{\partial \mathbf{f}_i}{\partial x} \mathbf{f}_r \mathbf{y}_j \frac{\partial \mathbf{y}_s}{\partial y} \right) \right] dx dy \end{aligned} \quad (7)$$

$$M_{ijrs} = E_{ir}^{(0,0)} F_{js}^{(0,0)} \quad (8)$$

$$E_{ir}^{(k,l)} = L^{(k+l-1)} \int_0^L \frac{\partial^k \mathbf{f}_i}{\partial x^k} \frac{\partial^l \mathbf{f}_r}{\partial x^l} dx; \quad F_{js}^{(k,l)} = B^{(k+l-1)} \int_0^B \frac{\partial^k \mathbf{y}_i}{\partial y^k} \frac{\partial^l \mathbf{y}_r}{\partial y^l} dy$$

It should be noted that in the equations above, the indices must be contracted to obtain the matrix eigenvalue problem in the standard form, as given by (5).

It should be also pointed out that the influence of the membrane stresses on the system dynamics is represented by the last term of equation (7), which is referred to as *initial-stress stiffness matrix*. As can be seen, this matrix is linear in the stress components.

### 3. The stress identification method (SIFDRIM)

*SIFDRIM* is a hybrid numerical/experimental method which explores the fact that stress state influences the dynamic responses. Stress identification is treated as a parameter identification problem, using parameterized models to represent the stress state. The identification is carried out by finding the values of the parameters that lead to the *minimum* value of a cost function that expresses the difference between model-predicted and experimentally measured natural frequencies (Vieira Jr. and Rade, 2003). To predict the dynamic responses taking into account the plate stress state, the Rayleigh-Ritz approach, developed in Section 2, is used. For optimization, *Genetic Algorithms* are used. In Figure (2), the block-diagram of the identification method is depicted.

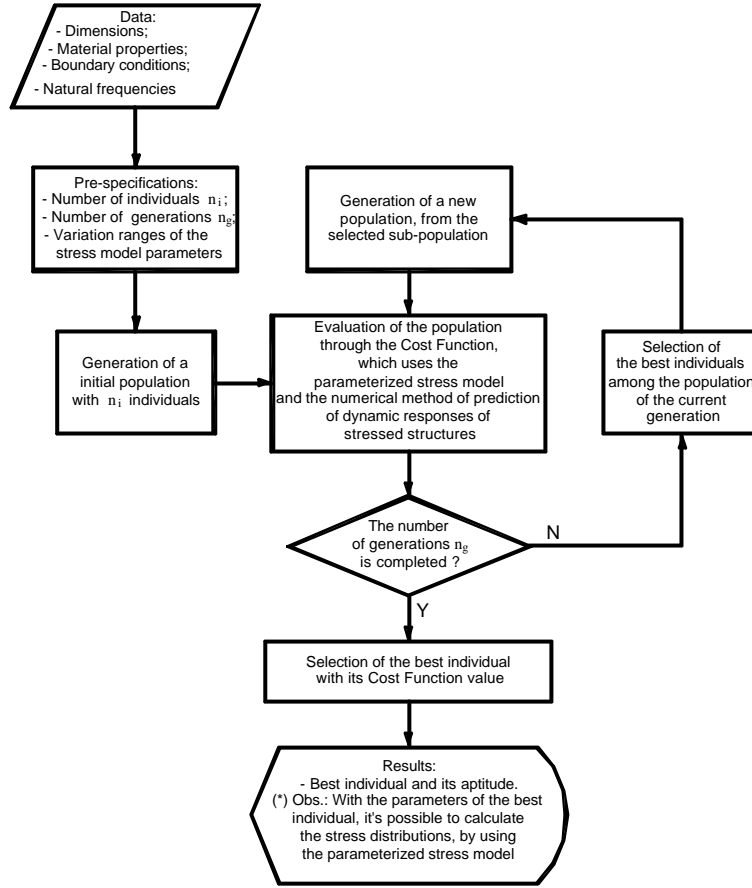


Figure 2. Block-diagram of the *SIFDRIM* ( Stress Identification from Dynamic Responses Inverse Method )

#### 4. Parameterized stress model for weld-induced residual stresses

The development of welding residual stresses can be mathematically modeled by the following differential equation (Kamtekar, 1978 ):

$$\nabla^4(U) = R \quad (9)$$

where:

$$- R = -E \left( \frac{\partial^2 \mathbf{e}_x^p}{\partial y^2} - 2 \frac{\partial^2 \mathbf{e}_{xy}^p}{\partial x \partial y} + \frac{\partial^2 \mathbf{e}_y^p}{\partial x^2} \right)$$

-  $\mathbf{e}_x^p$ ,  $\mathbf{e}_y^p$ ,  $\mathbf{e}_{xy}^p$  : Plastic strains;

$$- \nabla^4(\cdot) \equiv \frac{\partial^4(\cdot)}{\partial x^4} + 2 \frac{\partial^4(\cdot)}{\partial x^2 \partial y^2} + \frac{\partial^4(\cdot)}{\partial y^4}$$

-  $U = U(x, y)$ : Airy's stress function

Hence, upon knowing the plastic strain distributions, it is possible to calculate the Airy's stress function by solving equation (9) and, then, to obtain the distributions of the stress components through the relations:

$$\mathbf{s}_x = \frac{\partial^2 U}{\partial y^2}; \quad \mathbf{s}_y = \frac{\partial^2 U}{\partial x^2}; \quad \mathbf{t}_{xy} = -\frac{\partial^2 U}{\partial x \partial y} \quad (10)$$

In most of the cases, it is convenient to assess both Airy's stress function and stress components by using numerical methods, such as Finite Difference Technique.

It was observed from various numerical simulations, that for the case of welding, the right-hand side  $R$  of Eq. (9) often presents (with some approximation) the typical pattern shown in Fig. (3.a). In Figure (3.b), it can be seen how

this special feature can be explored in the development of a parameterized model of the right-hand-side term  $R$  in Eq.(1), which presents the very desirable characteristic of depending on a few parameters ( $p_1, p_2$  and  $p_3$ ). It is important to point out that the possibility of modeling the term  $R$  of Eq. (9) is equivalent to be able to model the Airy's stress function  $U$  and, as a result, the stress components  $s_x, s_y$  and  $t_{xy}$ . Nevertheless, this approach gives rise to the additional need of solving Eq. (9) by numerical procedures, such as the Finite Difference Method.

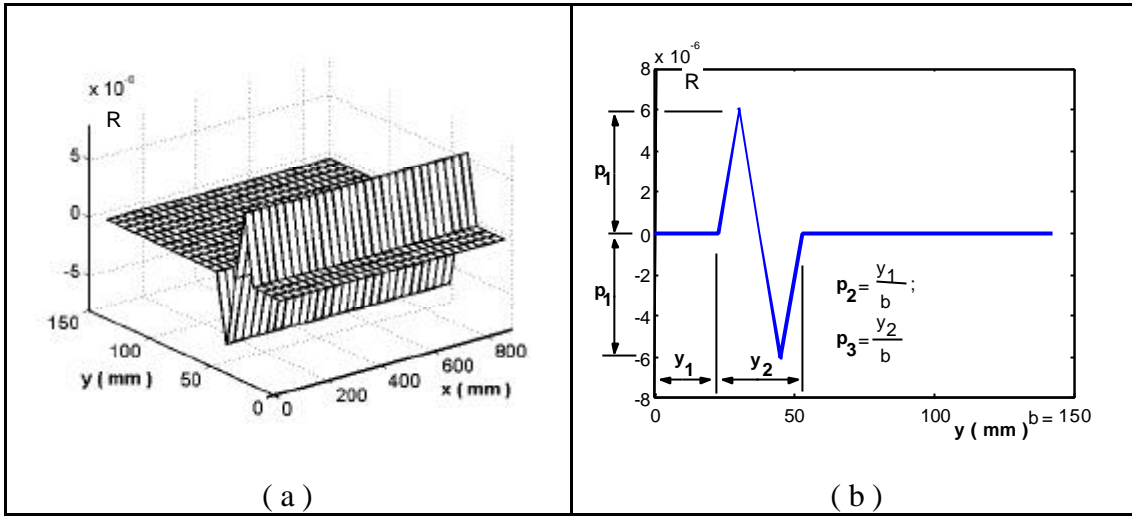


Figure 3. (a) – Proposed model for the distribution of the right-hand side  $R$  of Eq. (9); (b) – Characterization of the proposed parameterized model in terms of parameters  $p_1, p_2$  e  $p_3$

After the initial development of the three-parameter-model for  $R$ , it was proposed to introduce an additional parameter  $p_4$  which makes it possible to consider a function  $R$  that is not necessarily constant along the plate length ( $x$  axis). Each element of  $R$  in the finite-difference mesh, denoted by  $R_{ij}$ , must undergo a correction that depends on  $p_4$  which expresses the characteristic pattern of the variation of  $R$  with the  $x$  axis, according to Eq. (11). Figure (4) displays the shape of the correction matrix  $C$  along the  $x$  axis.

$$R_{ij} = (1 + p_4 C_{ij}) R_{ij}(p_1, p_2, p_3) \quad (11)$$

where:

$C_{ij}$  : correction coefficient applied to  $R_{ij}$ ;

$R_{ij}(p_1, p_2, p_3)$  : Element of the right-hand side  $R$  before the correction by  $p_4$  (like in Fig. (2.a))

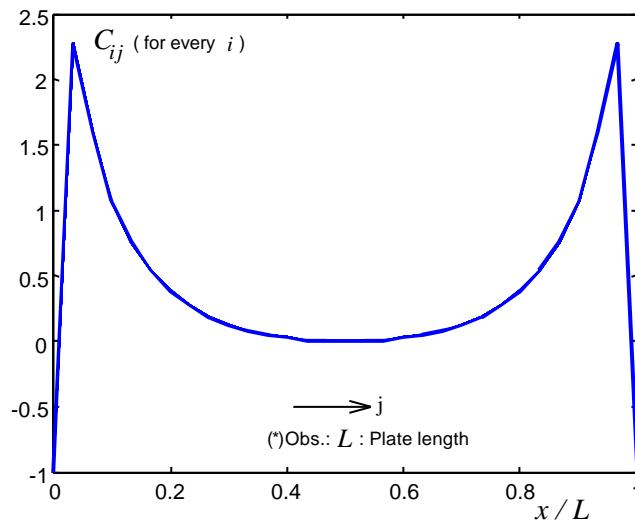


Figure 4. Shape of the correction matrix  $C_{ij}$  along the  $x$  axis

## 5. Application example

### 5.1 Studied case

As an application example of *SIFDRIM*, it was chosen the case studied by Kaldas and Dickinson (1981), of a  $254 \times 508 \times 3.175$  mm TIG (GTAW) welded plate. The dimensions, material properties and welding conditions are shown in Fig. (5). In that work, welding residual stress distributions were assessed by using numerical simulations based on the Finite Difference Technique. Those authors provided two-dimensional graphics of the stress components  $s_x$ ,  $s_y$  and  $t_{xy}$  along some specific plate sections (Fig. (6)). Natural frequencies were both numerically and experimentally obtained. In the numerical assessment, it was used the Rayleigh-Ritz Method. The numerically obtained and the experimental values of the ten first natural frequencies are listed in Table 1, considering two conditions concerning the stress state: stress-free and with welding residual stresses.

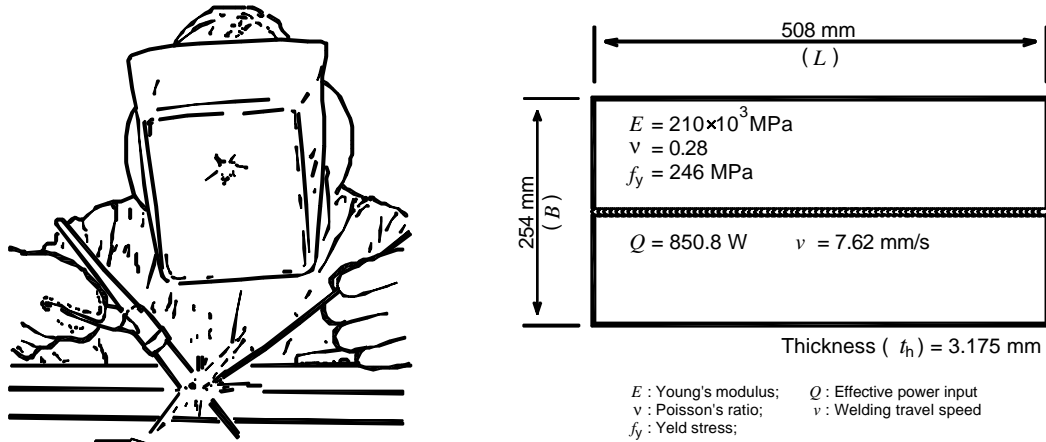


Figure 5. Plate dimensions, material properties and welding conditions (based on data provided by Kaldas and Dickinson, 1981)

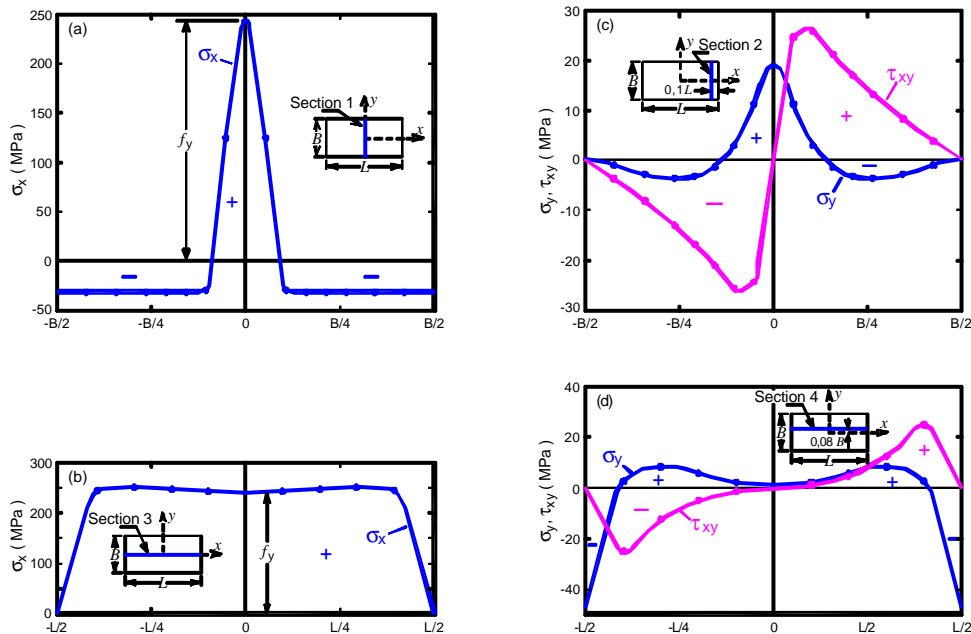


Figure 6. Welding residual-stress components along some sections of the welded plate (Kaldas and Dickinson, 1981)

Table 1 – Numerically and experimentally obtained natural frequencies (from (Kaldas and Dickinson, 1981))

Vibrating mode	Stress-free		With welding residual stresses	
	Numerically obtained (Hz)	Experimental (Hz)	Numerically obtained (Hz)	Experimental (Hz)
1	66.3	66.1	52.3	51.7
2	82.6	82.3	61.8	60.9
3	182.0	179.6	145.4	141.2
4	184.0	180.0	165.2	160.7
5	271.0	263.0	266.1	256.7
6	319.0	305.0	275.0	265.4
7	322.0	313.0	324.9	316.4
8	365.0	360.0	351.1	347.0
9	447.0	429.0	457.7	438.4
10	498.0	488.0	449.2	440.7

### 5.2 Initial estimates to the stress-model parameters

In order to estimate order of magnitude of parameters  $p_1, p_2$  and  $p_3$ . in practical welding conditions, one defines the following *dimensionless thermo-elasto-plastic coefficient* as follows:

$$a_{tep} = \frac{\mathbf{a} E}{f_y C_p} \frac{(Q/v)}{\mathbf{r} B t_h} \quad (12)$$

where:

- $\mathbf{a}$  : Thermal expansion coefficient;     $Q$  : Effective power input;     $\mathbf{r}$  : Density;
- $E$  : Young's modulus;     $v$  : Welding speed;     $B$  : Plate width;
- $f_y$  : Yield stress;     $C_p$  : Specific heat;     $t_h$  : Plate thickness

The following expressions, proposed by Vieira Jr. and Scotti (2003), given in Table 2, provide initial estimates of parameters  $p_1, p_2$  and  $p_4$  as functions of  $a_{tep}$ . No such approximation is available for parameter  $p_4$ .

Table 2 – Approximated values to the stress-model parameters as funtion of  $a_{tep}$

$a_{tep}$	Parameter	Approximation expression	Approximation
$a_{tep} = 0.4302$	$p_1$	$p_1 = 3.21 \times 10^{-6} a_{tep}^{2.39} \exp(-0.18 a_{tep}^{1.44})$	$p_1 = 4.05 \times 10^{-7}$
	$p_2$	$p_2 = 0.11 a_{tep}^{1.5} \exp(0.31 a_{tep})$	$p_2 = 0.03$
	$p_3$	$p_3 = 0.31 a_{tep}^{0.24}$	$p_3 = 0.25$

Based on the approximated parameter values, the following limits were set to the parameters variation ranges (Table 3). Some of the variation ranges were set with a tendency to the lower limit, since the approximation expressions were developed based on another welding process (Submerged Arc Welding) which uses higher welding energies.

Table 3. Variation ranges to the stress-model parameters

Parameter	Lower limit	Upper limit
$p_1$	$1 \times 10^{-7}$	$1 \times 10^{-4}$
$p_2$	0.00	0.05
$p_3$	0.20	0.30
$p_4$	0.20	0.40

### 5.3 Cost Function

The following cost function was defined so as to take into account the well-known steel-welding feature that Von-Mises stress, in the middle of the welding bead, is equal to the yielding stress limit.

$$F_{obj} = \frac{1}{n_f} \sum_{i=1}^{n_f} \left| \frac{f_i^c - f_i^m}{f_i^m} \right| + \frac{1}{100} \left| \mathbf{s}_e \left( \frac{L}{2}, 0 \right) - f_y \right| \quad (13)$$

where:

$F_{obj}$  : Cost function;

$n_f$  : Number of natural frequencies used as input data;

$f_i^c$  : i-th calculated natural frequency;

$f_i^m$  : i-th measured natural frequency;

$\mathbf{s}_e(L/2, 0)$ : Von-Mises stress in the middle of the welding bead;

$f_y$  : Yielding stress limit of steel (assumed value: 246 Mpa)

### 6. Results

Table 4 displays the stress-model parameter values obtained with *SIFDRIM*, and the setup numbers of individuals and generations used in the Genetic Algorithms program, as well as the final value of the Cost Function. Figures (7) and (8) show the graphics of stress components  $\mathbf{s}_x, \mathbf{s}_y$  and  $\mathbf{t}_{xy}$ , related to the identified stress-model parameters. For comparison, the same figures present the stress components resulting from welding numerical simulation, obtained by Kaldas and Dickinson (1981). Table 5 allows to compare the frequencies used as input data and those related to the identified stress state.

Table 4. Stress-model parameters obtained with *SIFDRIM*, Genetic Algorithms setup and final Cost Function value

Genetic Algorithms	Number of individuals	1000
	Number of generations	50
Identified parameters	$p_1$	$1.6231 \times 10^{-5}$
	$p_2$	0.0041
	$p_3$	0.2204
	$p_4$	0.2763
Final Cost Function value		0.0486

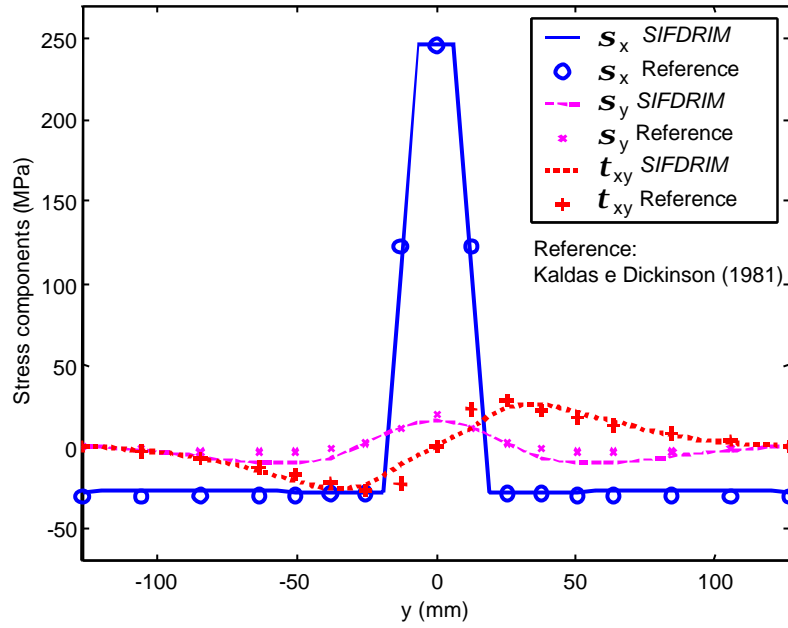


Figure 7. Comparison between the stress components obtained with *SIFDRIM* and those obtained by using welding numerical simulation (Kaldas e Dickinson, 1981). The stress components  $s_x$ ,  $s_y$  and  $t_{xy}$  are related to sections 1, 2 and 2, respectively (see Figure 2).

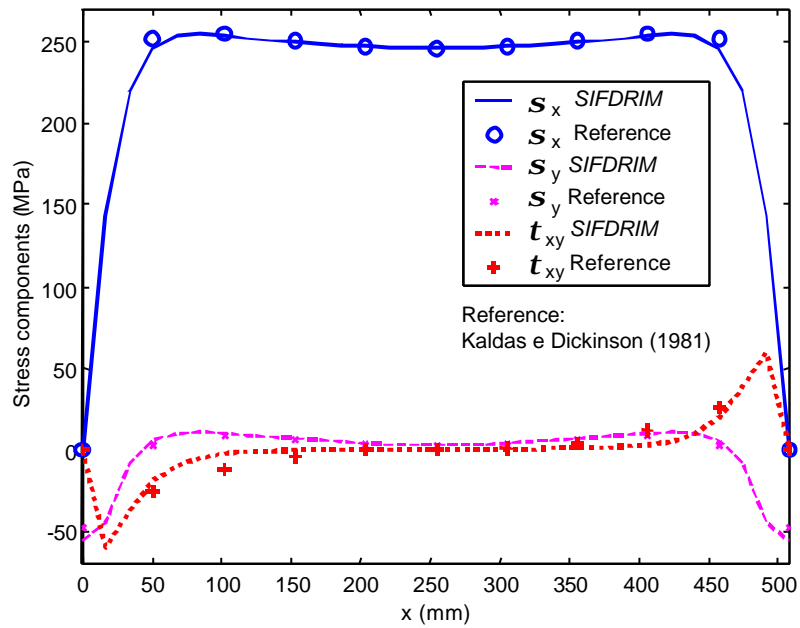


Figure 8 – Comparison between the stress components obtained with *SIFDRIM* and those obtained by using welding numerical simulation (Kaldas e Dickinson, 1981). The stress components  $s_x$ ,  $s_y$  and  $t_{xy}$  are related to sections 3, 4 and 4, respectively (see Figure 2).

Tabela 5. Comparison between calculated natural frequencies (related to the identified stress state) and the experimental values of natural frequencies used as input data

Vibrating mode	Natural frequencies (Hz)		Percent variation (%)
	Calculated	Experimental	
1	54.13	51.70	4.70
2	63.25	60.90	3.87
3	155.14	141.20	9.87
4	166.55	160.70	3.64
5	264.80	256.70	3.16
6	289.65	265.40	9.14
7	324.34	316.40	2.51
8	352.38	347.00	1.55
9	458.79	438.40	4.65
10	464.80	440.70	5.47

## 7. Concluding remarks

The results allows to conclude about the feasibility of applying the identification method *SIFDRIM* to the case of welding residual stress assessment. Good agreement was found between stress components obtained with *SIFDRIM* (using experimental natural frequencies of the welded plate) and those resulting of numerical welding simulations. Nevertheless, additional tests have shown that the problem of identification of welding residual stresses presents the characteristic of *non-unique solution*, which means that two different stress states can lead to the same set of natural frequencies. In the case of steel welding, this drawback can be easily overcome by considering, as an additional information, the fact that Von-Mises stress, in the middle of the welding bead, is equal to the yielding stress limit of the material. It is believed that the method can be extended to structures others than plates.

## 8. Acknowledgements

A.B. Vieira Jr., A. Scotti and D.A. Rade gratefully acknowledge agency CNPq of the Brazilian Ministry of Science and Technology for the grant of Ph.D. and research scholarships.

## 9. References

- Gérardin, M. and Rixen, D., 1997, *Mechanical Vibrations – Theory and Application to Structural Dynamics*, John Wiley & Sons, U.K., 425 p.
- Kaldas, M.M. and Dickinson, S.M., 1981, "Vibration and Buckling Calculations for Rectangular Plates Subject to Complicated In-Plane Stress Distributions by Using Numerical Integration in a Rayleigh-Ritz Analysis", *Journal of Sound and Vibration*, Vol.75, Num.2, Academic Press, U.K., pp. 151-152.
- Kamtekar, A.G., 1978, "The Calculation of Welding Residual Stresses in Thin Steel Plates", *International Journal of Mechanical Sciences*, Vol.20, Pergamon, U.K., pp. 207-227.
- Parlane, A.J.A., Allen, J.S., Harrison, J.D., Leggatt, R.H., Dwight, J.B., Bailey, N., Procter, E. and Saunders, G.G., 1981, "Residual Stresses and their Effect", *The Welding Institute*, U.K., 55p.
- Radaj, D., 1992, *Heat Effects of Welding; Temperature Field, Residual Stress, Distortion*, Springer-Verlag, Germany, 348 p.
- Vieira Jr., A.B., Cunha Jr., S.S. and Rade, D.A., 2002, "Avaliação Experimental da Influência das Tensões Residuais sobre as Respostas Dinâmicas de Placas Soldadas", II National Congress of Mechanical Engineering, CONEM2002, João Pessoa, PB, Brazil, Aug 2002, 10 p.
- Vieira Jr., A.B. and Rade, D.A., 2003, "Identification of Stresses in Plates from Dynamic Responses", IMAC-XXI: A Conference & Exposition on Structural Dynamics, Feb, 3-6, 2003, Orlando, FL, USA, 9p.
- Vieira Jr., A.B. and Scotti, A., 2003, "Modelamento da Distribuição das Tensões Residuais em Placas Soldadas", II Congresso Brasileiro de Engenharia de Fabricação, II COBEF, May, 18-21, 2003, Uberlândia, MG, Brazil, 10 p.

## 10. Copyright Notice

The author is the only responsible for the printed material included in his paper.